Rate and Driving Force for Protonation of Aryl Radical Anions in Ethanol[†]

Alison M. Funston, Sergei V. Lymar, Barbara Saunders-Price, Gidon Czapski, and John R. Miller*

Chemistry Department, Brookhaven National Laboratory, Upton, New York 11973

Received: February 20, 2007; In Final Form: March 30, 2007

Aryl radical anions created in liquid alcohols decay on the microsecond time scale by transfer of protons from the solvent.[1,2] This paper reports a 4.5 decade range of rate constants for proton transfer from a single weak acid, ethanol, to a series of unsubstituted aryl radical anions, Ar$^{-\bullet}$. The rate constants correlate with free energy change, $\Delta G°$, despite wide variations in the two factors that contribute to $\Delta G°$: (a) the reduction potentials of the aryls and (b) the Ar$-$H$^{\bullet}$ bond strengths in the product radicals. For aryl radical anions containing CH$_2$OH substituents, such as 2,2′-biphenyldimethanol$^{\bullet-}$ which is protonated with a rate constant of 3×10^9 s^{-1}, the faster rates do not fit well in the free energy correlation, suggesting a change in mechanism.

Introduction

Electron capture by molecules results in orders of magnitude increase in the basicity of the resultant radical anion relative to the neutral. Radical anions are therefore rapidly protonated even by weak proton donors, such as EtOH, to create neutral radicals. Pioneering studies by Dorfman[2] have shown that the protonation of several aryl radical ions by the solvent occurs on the millisecond to microsecond time scales in alcohols. In the gas phase, proton transfer by alcohols and other weak acids stabilizes unstable anions.[3] Free energy relationships have been reported for proton transfer from phenols to radical anions,[4] in (dimethylaniline$^{\bullet+}$, benzophenone$^{\bullet-}$) radical ion pairs,[5] or from weak acids to diphenylmethyl carbanions in dimethyl formamide (DMF)[6] that can be understood using theories of proton transfer.[7−9] With a single proton donor, ethanol (EtOH), Dorfman reported pseudo-first-order rate constants of up to ∼10^6 s^{-1}, but the energetics were not known and theory has not been applied to these reactions.[2] It may even be surprising that these reactions occur because acid dissociation constants for EtOH (pK_a = 29.8)[10] and the proton adduct, ArH$^{\bullet}$, of anthracene radical anion (pK_a = 23)[11] in dimethyl sulfoxide (DMSO) point to a endoergic proton transfer from EtOH to anthracene$^{-\bullet}$, although the reaction goes to completion with a rate of 4.0×10^5 s^{-1} in EtOH. This work observes several additional protonation reactions in EtOH with rates extending to the subnanosecond (3×10^9 s^{-1}) and provides estimates of energetics in EtOH leading to a free energy relationship for protonation of unsubstituted aryl radical anions. Protonation of the radical anions of biphenyls having CH$_2$OH (MeOH) ring substituents such as 2,2′-biphenyldimethanol appear to behave exceptionally, signaling a possible change in mechanism.

Experimental Section

Materials. Anhydrous tetrahydrofuran (THF, Aldrich, inhibitor-free, 99.9%) was distilled first from LiAlH$_4$ and then from sodium and benzophenone and subsequently stored under argon. Absolute ethanol (AAPER Alcohol and Chemical Co) was used as received in most experiments. For the experiments with terphenyl, pyrene, and biphenyl, in which protonations of the anion radicals were slow, ethanol was purified by distillation from CaH$_2$ and then from NaBH$_4$. The solvent quality was judged from the solvated electron half-life; it was 2.5 and 5.5 μs in commercial and purified ethanol, respectively; the latter compares well with the literature value of 6 μs.[12] Monodeuterated ethanol (EtOD) was distilled from NaBD$_4$. Aryl or aromatic compounds (all from Aldrich unless otherwise indicated with the stated purity in parentheses) were used as received: 2,2′-dimethylbiphenyl (97%), 2-methanolbiphenyl (99%), 4-methanolbiphenyl (98%), phenanthrene (99.5+%, zone-refined), pyrene (99%, optical grade), fluorobenzene, 1,5-dimethoxynaphthalene, naphthalene, [2,2]paracyclophane (99%), anthracene, and 4,4′-dimethoxybiphenyl (Biochemical Laboratories Inc.) were used as received. Biphenyl and xanthene were triply recrystallized, 2,2′-dimethanolbiphenyl (99%) was sublimed, and p-terphenyl (≥99%) was zone-refined prior to use. Sodium ethylate was prepared by dissolving NaOH in purified EtOH followed by centrifugation to remove a small amount of insoluble carbonate; the resulting clear, colorless 1 M NaEtO stock solution was stored under nitrogen. Although an equivalent amount of water is produced in this preparation, we estimate from the data of Caldin and Long[13] that over 93% of the total base is present as EtO$^-$ rather than OH$^-$.

Pulse Radiolysis. Pulse radiolysis was employed to generate the aryl radical anions. Fast electrons ionize the condensed media (reaction 1) to form solvent radical cations (RH$^{\bullet+}$) and secondary electrons that quickly become solvated to form solvated electrons, e^-_s. In both ethanol and THF, the solvent radical cation (RH$^{\bullet+}$) rapidly (less than ∼1 ps) transfers a proton to a neighboring solvent molecule (reaction 2), creating a radical (R$^{\bullet}$) and a solvated proton (RH$_2^+$).
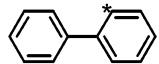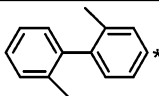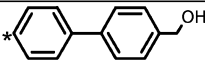
$$RH \rightsquigarrow RH^{\bullet+} + e^-_s \qquad (1)$$

$$RH^{\bullet+} + RH \rightarrow R^{\bullet} + RH_2^+ \qquad (2)$$
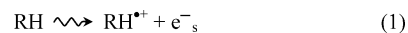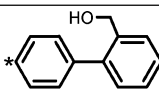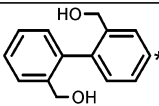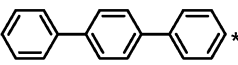
Under our experimental conditions, solvated electrons are the only species that generate the radical anions of aromatic solutes.

The slower kinetic and transient spectra measurements were carried out with pulses of 2 MeV electrons from a van de Graaff (VDG) accelerator; pulse widths were in the range 60−300 ns.

TABLE 1: Rate and Absorption Data Pertinent to Protonation of Aryl Anion Radicals[a]
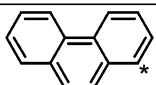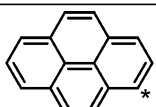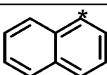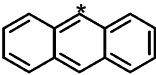
Aryl[b]		$k_3 \times 10^{-9}$ (Ar + e_s^-)	$\lambda_{max}(Ar^{\bullet-})$, nm	k_4 (Ar$^{\bullet-}$ + EtOH)	$\lambda_{max}(ArH^{\bullet})$, nm
	biphenyl	4.3 ± 0.7^{c}	630, 400	$2.8 \times 10^{5\ d}$	310^{f}, 320^{g}
	2,2'-dimethyl biphenyl		780, 400	4.2×10^{7}	
	4-biphenyl methanol		650, 400	2.9×10^{7}	
	2-biphenyl methanol		675, 400	4.7×10^{7}	
	2,2'-biphenyl dimethanol	1.5 ± 0.1	780, 375	$3.0 \times 10^{9\ c}$	325^{f}
	p-terphenyl	7.2 ± 0.6	906, 470	$1.1 \times 10^{3\ d}$	
	phenanthrene		1140, 450	3.3×10^{6}	390^{f}, 400^{g}
	pyrene	8.5 ± 0.8	500, 380	1.1×10^{4}	400^{f}
	naphthalene	5.4 ± 0.5^{c}	800, 365	5.0×10^{6}	$330^{f,g}$
	anthracene	16	367, 720	$4.0 \times 10^{5\ e}$	

[a] Rate constants are in M^{-1} s^{-1} for electron scavenging and in s^{-1} for pseudo-first-order protonation in neat EtOH. Except where indicated, all rates and λ_{max} for Ar$^{\bullet-}$ and ArH$^{\bullet}$ are measured in this work. Uncertainties in rates are ±15%. [b] Asterisks show the most probable protonation site based on free energy calculations (see Supporting Information Table S1). [c] ±25%. [d] Dorfman[2] gives 4.4×10^5 and 4×10^2 s^{-1} for biphenyl and *p*-terphenyl, respectively. [e] Arai.[21] [f] Present results. [g] Fendler;[22] these results did not permit reliable determinations of extinction coefficients.

Three passes of analyzing light through a 2 cm cell were used in the detection optical path. For the kinetics recorded on a time scale of less than 100 μs, the analyzing xenon arc light source was pulsed. Except for the temperature dependence studies, all VDG experiments were performed with temperature stabilization at 25 ± 1 °C in Ar-purged solutions. Dosimetry was performed with N$_2$O-saturated 10 mM KSCN aqueous solution using $G\epsilon = 4.87 \times 10^4$ ions (100 eV)$^{-1}$ M^{-1} cm^{-1} for the (SCN)$_2^{\bullet-}$ radical at 472 nm.

Nanosecond and picosecond measurements were carried out at the Brookhaven National Laboratory Laser-Electron Accelerator Facility (LEAF).[14] Transient absorption was measured using an FND-100Q silicon diode ($\lambda \leq 1000$ nm, 2 ns rise time) with a Tektronix 680B digitizer or an R1328-03 biplanar phototube with a Tektronix 694C transient digitizer (300–700 nm, 0.3 ns system rise time). A pulse–probe method, analogous to the laser pump–probe technique, gave 17 ps time resolution. The nanosecond measurements utilized a 2 cm cell, a 75 W xenon pulsed arc lamp, and wavelength selection with 40 or 10 nm bandwidth interference filters. For nanosecond

measurements carried out in ethanol, dissolved oxygen was removed by purging the solution with argon gas for at least 10 min prior to use; then, the cells were sealed with septa. For measurements in THF, samples were prepared under an argon atmosphere and sealed using Teflon stopcocks. The dose per pulse was determined before each series of experiments by measuring the transient absorption of the hydrated electron in water using $\epsilon(e^-_{aq}) = 18.5 \times 10^3$ M^{-1} cm^{-1} at 700 nm and $G(e^-_{aq}) = 2.97$ molecules/100 eV at 10 ns. In pulse–probe measurements, the transient absorbance is probed at a single time delay relative to each accelerator pulse, requiring a few thousand pulses to obtain a kinetic trace and using about 50 mL of solution flowing through a 1 cm cell. The absorption–time data were analyzed with IGOR Pro software (Wavemetrics). Reaction rate constants were determined using a nonlinear least-squares fitting procedure described previously.[15] Uncertainties for rate constants are quoted as ±2σ of the rate parameter of the fit. Where not stated, uncertainties are 15%.

Radiation doses of 5–20 Gy were employed. Correction factors of 0.80 and 0.89 were applied to account for lower

Protonation of Aryl Anions

J. Phys. Chem. B, Vol. 111, No. 24, 2007 **6897**

TABLE 2: Protonation Energetics of Aryl Anion Radicals (in eV/molecule)

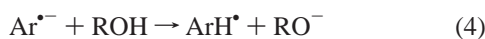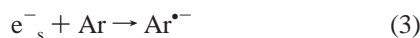| aryl	$\Delta_d H^a$	$\Delta_d G^a$	$E°(Ar/Ar^{\bullet-})^b$	$\Delta G° - X^c$
biphenyl	1.13	0.85	−2.60	−0.03
2,2′-dimethyl biphenyl	1.05	0.74	−2.94	−0.26
4-biphenyl methanol	1.14	0.85	−2.63	−0.06
2-biphenyl methanol	1.10	0.75	−2.67	−0.00
2,2′-biphenyl dimethanol	1.06	0.76	−2.92	−0.26
p-terphenyl	1.16	0.85	−2.28^d	0.29
phenanthrene	1.30	0.99	−2.47	−0.04
pyrene	1.52	1.22	−2.08	0.12
naphthalene	1.36	1.07	−2.54	−0.19
anthracene	1.85	1.60	−1.96	−0.14
benzene	1.03^e	0.73^e	−3.25	−0.56

^{a} Refers to the bond dissociation energies ArH$^\bullet$ → Ar + H$^\bullet$ computed by B3LYP/6-31G(d). ^{b} Reduction potential in V of Ar vs SCE,[23] or measured in this work. ^{c} Free energy change for proton transfer (reaction 4). The term X contains uncertainties of the origin (see eq 10) and is estimated to be ≤ −0.28 eV. ^{d} Reduction potential −2.40[24] vs Ag/AgCl adjusted to SCE reference. ^{e} Experimental values[25] are $\Delta_d H = 0.92$ and $\Delta_d G = 0.67$ eV with ±0.13 eV uncertainties.

radiation energy absorption in ethanol and THF, respectively, relative to the aqueous dosimeters. A product of $G\epsilon = 1.57 \times 10^4$ electrons (100 eV)$^{-1}$ M^{-1} cm^{-1} for e^-_s at 700 nm was obtained for neat ethanol in agreement with literature values.[12] All spectra and molar extinction coefficients of the aryl radicals were calculated under conditions of complete scavenging of e^-_s and using $G(e^-_s) = 1.7$ for ethanol[12,16] and 0.53 electrons per 100 eV for THF (the average of a number of reported values).[17] Samples were prepared immediately prior to use. During irradiation, samples were exposed to as little UV light as possible via the use of UV cutoff filters to avoid photodecomposition. No evidence of photodecomposition was found within the time frames monitored. Except for temperature-dependent experiments, measurements at LEAF were carried out at 21 °C. Some measurements were made at the 20 MeV Linac at Argonne National Laboratory using an experimental setup described previously.[15]

Density Functional Theory (DFT). DFT calculations were performed using Gaussian 03[18] using the B3LYP functional.[19] Geometries of molecules were optimized first by AM1 followed by optimization by DFT using the B3LYP functional. Semiempirical Zindo/S calculations of spectra with AM1 optimizations were performed in Hyperchem 7 as were screening optimizations.

Results

Solvated electrons react with aromatic solutes (Ar) to produce their radical anions (Ar$^{\bullet-}$, reaction 3), which are strong bases that may be protonated to form the neutral radicals (ArH$^\bullet$, reaction 4). The neutral radicals decay via radical−radical reactions (e.g., reaction 5).

$$e^-_s + Ar \rightarrow Ar^{\bullet-} \quad (3)$$

$$Ar^{\bullet-} + ROH \rightarrow ArH^\bullet + RO^- \quad (4)$$

$$ArH^\bullet + ArH^\bullet \rightarrow products \quad (5)$$

Rate constants for the reaction of e^-_s with aromatic solutes and the subsequent reaction of the aromatic radical anions and the solvent, reactions 3 and 4, for the aromatic molecules investigated in ethanol are summarized in Table 1, along with the spectral maxima of the radical anions and protonated radicals, ArH$^\bullet$. The reduction potentials for the aromatic solutes are compiled in Table 2. Electron attachments are typically
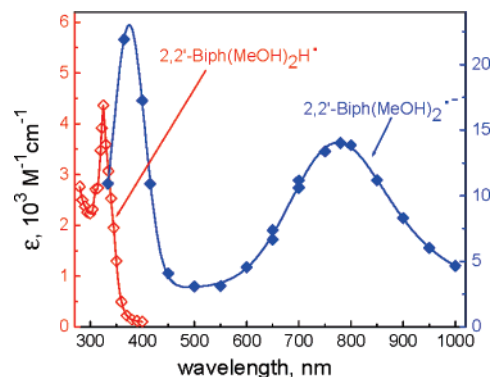

Figure 1. (◆) Absorption spectrum (right axis) of 2,2′-biphenyldimethanol radical anion in a THF solution containing 0.21 M 2,2′-biphenyldimethanol measured at 10 ns following the electron pulse. (◇) Absorption spectrum of the protonated radical upon completion of reaction 4 in Ar-saturated ethanol solution containing 2.6 mM 2,2′-biphenyldimethanol; each point is an average of at least three runs.
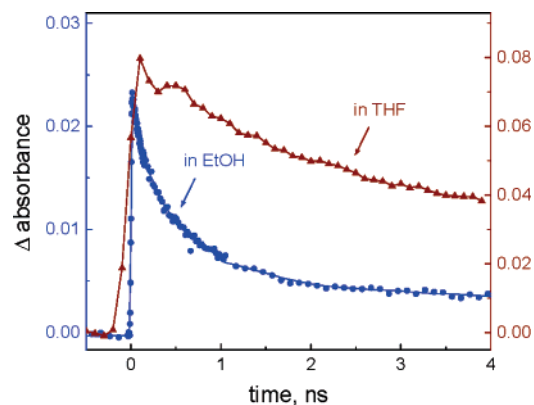

Figure 2. Kinetics of decay of the radical anion observed at 400 nm (●) in ethanol by pulse−probe and (▲) in THF measured with the R1328-03 phototube and Tektronix 694C transient digitizer. Concentrations of 0.4 and 0.5 M 2,2′-biphenyldimethanol were used in the two cases.

diffusion-controlled for the more exoergic reactions but somewhat slower for weakly exoergic attachments, particularly that of 2,2′-biphenyldimethanol. The two bulky 2-methanol substituents on 2,2′-biphenyldimethanol force the anion to be somewhat nonplanar, which in turn is likely to cause the very negative reduction potential. It is apparent from this data that, for the aromatics investigated, the protonation rate of the radical anion by EtOH, k_4, spans more than 6 orders of magnitude and there is a nearly four decade increase in the protonation rate (reaction 4) for the 2,2′-biphenyldimethanol radical anion over that for biphenylide.

Optical absorption spectra of many aromatic radical anions have been reported previously.[2,20] The absorption spectrum of the radical anion of 2,2′-biphenyldimethanol in THF is shown in Figure 1, along with that of the product radical. A partial spectrum of the radical anion in ethanol, where the 0.3 ns lifetime of the anion precludes accurate measurements at many wavelengths, is identical to that in THF. Figure 2 displays decay kinetics of the 2,2′-biphenyldimethanol anion in ethanol and THF. The spectra for radical anions of the other substituted biphenyls investigated in ethanol are shown in Figure 3; the well-known spectra for unsubstituted biphenyl are in the Supporting Information.

The protonation of methanol-substituted biphenyls in THF may occur by intermolecular (reaction 6) and intramolecular
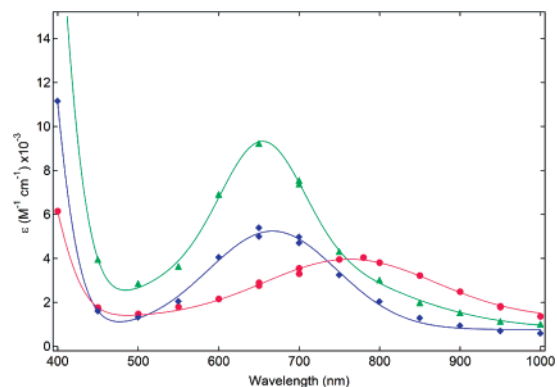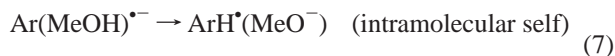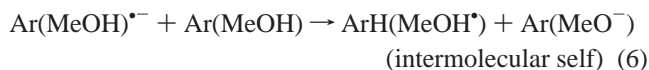
Figure 3. Absorption spectra of radical anions of 2-methanolbiphenyl (0.51 M) (◆), 4-methanolbiphenyl (0.55 M) (▲), and 2,2′-dimethyl-biphenyl (0.48 M) (●) in ethanol at 12, 20, and 10 ns, respectively, after the electron pulse.

(reaction 7) self-protonation; these rates are reported in Table 3. Intramolecular protonation rates for 2- and 4-biphenylmethanol are indistinguishable from zero.

$$Ar(MeOH)^{\bullet-} + Ar(MeOH) \rightarrow ArH(MeOH^\bullet) + Ar(MeO^-)$$
$$\text{(intermolecular self)} \quad (6)$$

$$Ar(MeOH)^{\bullet-} \rightarrow ArH^\bullet(MeO^-) \quad \text{(intramolecular self)} \quad (7)$$

An attempt to extract inter- and intramolecular rates from dependence of rate on 2,2′-biphenyldimethanol concentration in ethanol was not successful, as the rates can be measured to reasonable accuracy only over a narrow range of high concentrations.

Prompt capture of electrons by 2,2′-biphenyldimethanol aided the measurement of proton transfer in its anion. At the highest aryl concentration used, 0.5 M, the 1.5×10^9 M^{-1} s^{-1} rate constant for electron capture is expected to cause conversion of only 1.4% of e^-_s to anions within 17 ps, the instrument response time. By contrast, pulse−probe measurements at 400 nm, where e^-_s absorbs little, showed instead that $70 \pm 20\%$ of electrons were converted to anions by 17 ps; the uncertainty in the yield arises principally from uncertainties in the relative extinction coefficients. This efficient early time conversion, not accounted for by the reaction kinetics of the aryl molecule with the solvated electron, is due to the reaction of "presolvated" electrons, that is, those electrons not yet solvated, with the 2,2′-biphenyldimethanol and allows determination of the rate of protonation of the 2,2′-biphenyldimethanol radical anion by ethanol.

Reduction potentials in aprotic solvents are available from electrochemical measurements for many of the aryls studied here (see Table 2) but not for those having methanol groups, which makes the radical anions short-lived (cf. Table 3). The reduction potentials for these aryls were obtained from bimolecular electron transfer equilibria between the methanol-containing molecule and an acceptor having a known, reversible reduction potential. The equilibria, established on the nanosecond time scale, were measured by pulse radiolysis in THF. For 2,2′-biphenyldimethanol, only upper and lower bounds for the potential could be reliably determined, as shown in Supporting Information Figure S1.

The product of reaction 4 is an ArH$^\bullet$ radical. In those cases when the ArH$^\bullet$ spectra could be observed, the decay kinetics could be measured. This has been carried out for the two ArH$^\bullet$ at each end of the protonation rate range. In both cases, the radical decay obeys a second-order rate law, as evident from

the apparent rate constant dependence on the radiation dose (Figure 4). These features suggest a simple self-recombination (reaction 5) for the decay. Assuming the radiation yield $G(ArH^\bullet)$ = $G(e^-_s)$ = 1.7,[12] the same recombination rate constant, $2k_5$ = $(4.3 \pm 0.2) \times 10^9$ M^{-1} s^{-1}, is derived for both 2,2′-biphenyldimethanol and pyrene H-atom adducts. It would thus appear that reaction 5 is essentially diffusion-controlled. Notably, in both cases, there are essentially the same and significant ($\sim 1 \times 10^3$ s^{-1}) intercepts evident. These intercepts indicate that, in addition to reaction 3, there exists an approximately first-order channel for the ArH radical decays. Possibilities include reactions of ArH$^\bullet$ with the more numerous solvent radicals or with impurities, possibly with traces of oxygen.

For those Ar$^{\bullet-}$ that are protonated by EtOH sufficiently slowly, the second-order decay (reaction 5) interferes with the observations of the ArH$^\bullet$ radical formation, and observation of its spectrum, even at very low doses. For instance, as is obvious from Figure 5, the decay has to be accounted for when determining the molar absorptivity of the pyrene protonated radical, PyrH$^\bullet$. With *p*-terphenyl, the protonation of the radical anion is so slow that the protonated radical could not be observed at all and the protonation rate was inferred from the anion radical first-order decay rate only; early and late spectra are in Supporting Information Figure S5.

Temperature Dependence and Kinetic Isotope Effect. A fairly low activation energy of 3.1 kcal/mol and preexponetial factor of 6.7×10^7 s^{-1} were previously reported[1] for protonation of biphenyl anion in ethanol; we have confirmed these numbers (Figure 6 and Table 4). The nearly four decade increase in protonation rate for the 2,2′-biphenyldimethanol radical anion over that for biphenylide is not readily accounted for by a decrease in activation energy, E_a, alone. As shown in Figure 6 and Table 4, we find that activation energy is slightly larger for the 2,2′-biphenyldimethanol anion, contrary to the expectation that larger activation energies lead to slower rates. Another salient dissimilarity of the two aryls is in the kinetic isotope effect (KIE) expected for a proton transfer reaction. Whereas for biphenylide we observe a normal primary KIE, KIE = k_4(H)/k_4(D) = 14.7 at 22 °C, the KIE is practically absent for the dimethanol derivative, KIE = 1.9. For naphthalene, a measurement at room temperature gives a KIE of 4.2.

Discussion

Protonation Rates. While the structure of 2,2′-biphenyldimethanol appears conducive to intramolecular protonation, that process occurs with a rate constant of only 3.1×10^7 s^{-1} in THF. If the rate of intramolecular protonation in EtOH is similar to that in THF, then most (>99%) of the 3.0×10^9 s^{-1} rate in ethanol is due to protonation by ethanol solvent (reaction 4). Intramolecular protonation would produce a product having one MeO$^-$ subustituent, but spectral changes might be small, and have not been observed here. The MeO$^-$ may also be quickly reprotonated by solvent. Intramolecular proton transfer should also be possible in anions of 2-biphenylmethanol but should occur negligibly, if at all, in anions of 4-biphenylmethanol. The rates of intramolecular proton transfer for both anions in THF are zero within experimental uncertainty (Table 3). The lack of concentration dependence of the determined rates in ethanol shows that intermolecular protonation in ethanol is also a minor route.

The rates of protonation of the various Ar$^{\bullet-}$ radical anions by ethanol (reaction 4) span 6.5 decades (Table 1); the k_4 = 3.0×10^9 s^{-1} rate for 2,2′-biphenyldimethanol is almost 4

TABLE 3: Electron Attachment and Protonation Rate Constants for Substituted Biphenyls in THF[a]

aryl	$k(e^-_s + aryl)$	k_7, s^{-1} intra	k_6, M^{-1} s^{-1} inter
2,2′-biphenyldimethanol	$(1.2 \pm 0.3) \times 10^{11}$	$(3.1 \pm 0.4) \times 10^7$	$(4.2 \pm 0.2) \times 10^8$
2-biphenylmethanol	$(4.1 \pm 0.8) \times 10^{10}$	$(1.5 \pm 2) \times 10^5$	$(1.3 \pm 0.1) \times 10^7$
4-biphenylmethanol	$(4.5 \pm 0.3) \times 10^{10}$	$(0.5 \pm 3) \times 10^5$	$(3.7 \pm 0.1) \times 10^7$

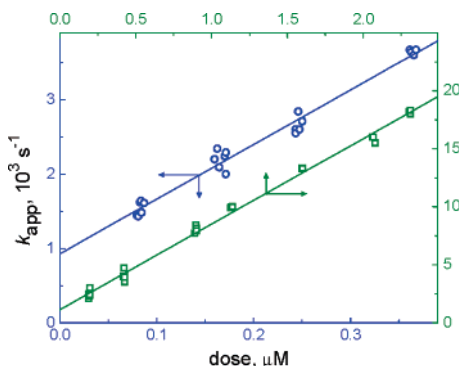[a] Rates are corrected for other decay processes such as reactions of anion with other radicals.

Figure 4. Dependence upon the radiation dose of the apparent rate constants, $k_{app} = 2k_5[ArH^\bullet]_0$, for the second-order decays through reaction 5 in ethanol: (□, top and right axes) 2,2′-biphenyl dimethanol; (○, bottom and left axes) pyrene. The dose is expressed as the concentration per unit G value produced per pulse. The solid lines show linear fits to the data.

decades faster than that for unsubstituted biphenyl, $k_4 = 4.4 \times 10^5$ s^{-1}. The rate for the structurally related p-terphenyl (which can be viewed as para-substituted biphenyl) is lower further by 2.5 decades. These dramatic differences are compared with overall reaction energetics in Figure 7.

Energetics of Protonation. The energetics of the proton transfer were evaluated by breaking reaction 4 into two half-cell redox reactions. The first involves reduction of ethanol

$$\text{EtOH}_{\text{EtOH}} + e^- = \text{EtO}^-_{\text{EtOH}} + \text{H}^\bullet_{\text{gas}} \qquad (8)$$

with the subscripts indicating the medium. From the literature thermochemical data, the standard reduction potential $E_8 = -3.42$ V vs SCE is obtained (see the Supporting Information). The second redox reaction is aryl-specific

$$\text{ArH}^\bullet_{\text{EtOH}} + e^- = \text{Ar}^{\bullet-}_{\text{EtOH}} + \text{H}^\bullet_{\text{gas}} \qquad (9)$$

If the reduction potential, E_9, for this half-cell is evaluated against the same reference (SCE is chosen here), then $\Delta G° = E_9 - E_8$ for reaction 4 (with $\Delta G°$ in electronvolts), and the so-obtained $\Delta G°$ values are used to correlate the rates with energetics in Figure 7. The values for E_9 were calculated from the measured reduction potentials for aryls, $E°(\text{Ar}/\text{Ar}^{\bullet-})$, and computed gas phase Ar−H bond dissociation free energies for the ArH$^\bullet$ radicals, $\Delta_d G$, collected in Table 2; that is, $E_9 = E°(\text{Ar}/\text{Ar}^{\bullet-}) - \Delta_d G + X$, with all values in volts (see the Supporting Information for derivation details). The X term includes a liquid junction potential and the free energies for phase transfers that are not known but are presumed to be the same for all aryls used in this work. As discussed below, the value for this term is negative, $X \leq -0.28$ eV. Thus, for the free energy change in Ar$^{\bullet-}$ protonation by EtOH, we obtain

$$\Delta G° = E°(\text{Ar}/\text{Ar}^{\bullet-}) - \Delta_d G + X + 3.42 \text{ eV} \qquad (10)$$

and the values of $\Delta G° - X$ are given in Table 2. If the undetermined X were zero or small, our analysis predicts protonations of pyrene$^{\bullet-}$ and p-terphenyl$^{\bullet-}$ to be slightly

endergonic, and it should be possible to determine X by establishing protic equilibrium between Ar$^{\bullet-}$ and EtO$^-$. In the hope of directly determining the equilibrium constants for reaction 4, we measured the protonation rates of pyrene$^{\bullet-}$ and p-terphenyl$^{\bullet-}$ in ethanol containing various concentrations of NaEtO. Should the equilibration occur, the observed rates of Ar$^{\bullet-}$ decay would increase by a factor of $1 + [\text{EtO}^-]/(K_4[\text{EtOH}])$ and the decay of Ar$^{\bullet-}$ would not go to completion. Neither of these effects was observed. The data in Figure 8 clearly show that the observed protonation rate actually slightly decreases with [EtO$^-$], which could be simply an ionic strength effect. Assuming that a 10% rate increase would be detectable, we estimate $K_4 > 10[\text{EtO}^-]_{\text{max}}/[\text{EtOH}] \approx 0.56$. This result shows that the X term is negative; from $\Delta G° - X$ in Table 2, $X \leq -0.28$ eV. This limit on the X term was applied to Figure 7 by using -0.28 eV for X in eq 10. In contrast to the equilibration lifetime, the observed radiation yields of Ar$^{\bullet-}$ markedly increase with solution alkalinity, doubling at ~1 M NaEtO (Figure 8). A quantitatively similar yield increase has been observed previously for p-terphenyl$^{\bullet-}$ and explained by the suppression of the geminate and spur recombination of e^-_s and H$^+$ due to the rapid H$^+$ + EtO$^-$ reaction;[26] our data are consistent with this interpretation.

Free Energy Relation. Figure 7 shows that the protonation rate depends on $\Delta G°$ and is sensitive to both of the aryl-specific contributions in $\Delta G°$. Two plots shown in Supporting Information Figures S1 and S2 for the protonation rates vs $E°(\text{Ar}/\text{Ar}^{\bullet-})$ and vs $\Delta_d G(\text{ArH}^\bullet)$ exhibit substantially more scatter than Figure 7. The free energy relation found here accounts for interesting features of the data. The rate of protonation of biphenyl$^{\bullet-}$ ($E° = -2.6$ V) is ~240-fold faster than that of p-terphenyl$^{\bullet-}$ ($E° = -2.28$ V), supporting the notion that more stable anions (less reducing) resist protonation. On the other hand, the rate for anthracene$^{\bullet-}$ ($E° = -1.96$ V) is nearly the same as that for biphenyl$^{\bullet-}$, despite the more than 0.6 V difference in reduction potentials. The similarity of the two rates can be understood on the basis of the opposing effect of $\Delta_d G$-(ArH$^\bullet$) which is 0.75 eV larger for anthracene. Still, there is scatter in the plot of rate vs $\Delta G°$; especially points for the MeOH-substituted biphenyls all appear to lie above, or to the left of, the trend. Their higher rates, which may signal a change in mechanism, will be discussed separately below. The small but positive activation energies for two reactions (Table 4) were simultaneously included in the fit using eq 13.

Reaction Barriers. Although appearing to be first-order, protonation by solvent is a bimolecular reaction that includes two steps, the precursor complex formation and the proton transfer itself. The first step does not involve diffusion, but it does require a reorientation of EtOH and Ar$^{\bullet-}$ so that the hydroxylic H atom is aligned with the donor O and the acceptor C atoms, a process that will eventually become rate-limiting for sufficiently high overall rates. However, it has been recently shown that protonation of nonaromatic carbon of strongly basic diphenylcarbene (Ph$_2$C) occurs in some 15 ps in neat EtOH,[27] which is over an order of magnitude more rapid than the fastest rate observed in this work. It is thus reasonable to assume that all protonation rates in Figure 7 are kinetically controlled by
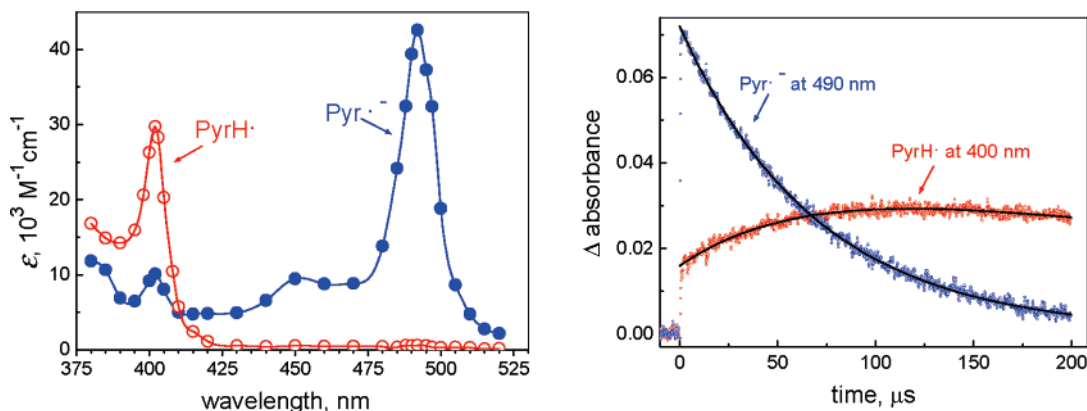
Figure 5. (left panel) Absorption spectra for anions and protonated radicals of pyrene in ethanol. Each point is an average of at least three runs. The Pyr$^{\bullet-}$ spectrum is that appearing immediately after the pulse. The PyrH$^{\bullet}$ spectrum is obtained by fitting the kinetic traces of its simultaneous formation and decay; the spectrum so obtained should well approximate the "true" PyrH$^{\bullet}$ spectrum. Addition of ethoxide removes the small peak at 400 nm in the Pyr$^{\bullet-}$ spectrum, showing that it actually belongs to a few PyrH$^{\bullet}$ radicals (see Supporting Information Figure S4). (right panel) Kinetics traces showing Pyr$^{\bullet-}$ decay at 490 nm and PyrH$^{\bullet}$ formation at 400 nm following pulse radiolysis of Ar-saturated 2.2 mM pyrene in EtOH with a dose of 0.16 μM per unit G value. For the Pyr$^{\bullet-}$ decay, the line gives an exponential fit with a 1.44×10^4 s^{-1} rate constant. For the PyrH$^{\bullet}$ kinetics, the line shows a biexponential fit with 1.44×10^4 s^{-1} formation and 2.19×10^3 s^{-1} decay rate constants, respectively.
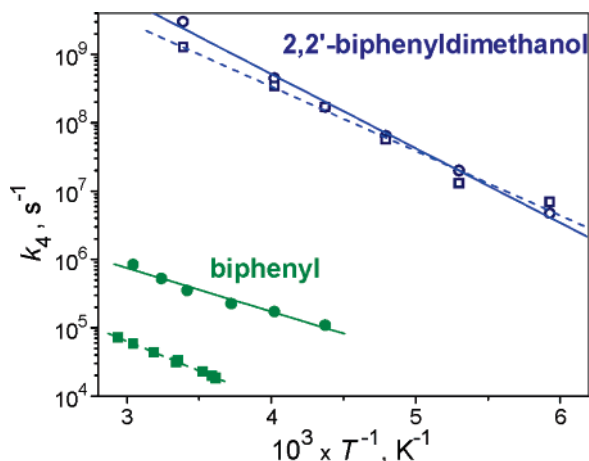

Figure 6. Temperature dependencies of the protonation rate constants for the 2,2′-biphenyldimethanol radical anion (open symbols) and for the biphenyl radical anion (closed symbols) in EtOH (circles) and in EtOD (squares). The lines show the linear fits to the data.

TABLE 4: Arrhenius Activation Parameters^a for the Protonation Rates

	EtOH		EtOD	
aryl	$\log(A,\ s^{-1})$	E_a, meV	$\log(A,\ s^{-1})$	E_a, meV
biphenyl	7.8 ± 0.2^b	126 ± 13^b	7.4 ± 0.1	174 ± 4
2,2′-biphenyl dimethanol	13.1 ± 0.2	217 ± 9	12.3 ± 0.3	187 ± 13

^{a} Uncertainties are given as standard errors for the linear fits in Figure 6. ^{b} Dorfman and co-workers[1] give $\log A = 7.8$ and $E_a = 134$ meV. For anthracene, $E_a = 113$ meV.[1]

free energy barriers, $\Delta G^{\ddagger}$:

$$k_4 = \nu \exp(-\Delta G^{\ddagger}/kT) \qquad (11)$$

$$\nu = kT/h \qquad (11a)$$

or

$$\nu = \kappa \nu_0 = (2\pi C^2/h)(\pi/\lambda kT)^{1/2} \qquad (11b)$$

The nature of the frequency factor, ν, depends upon whether the reaction occurs in the adiabatic (eq 11a) or nonadiabatic[9] (eq 11b) regime. In eq 11b, C is a proton tunneling matrix
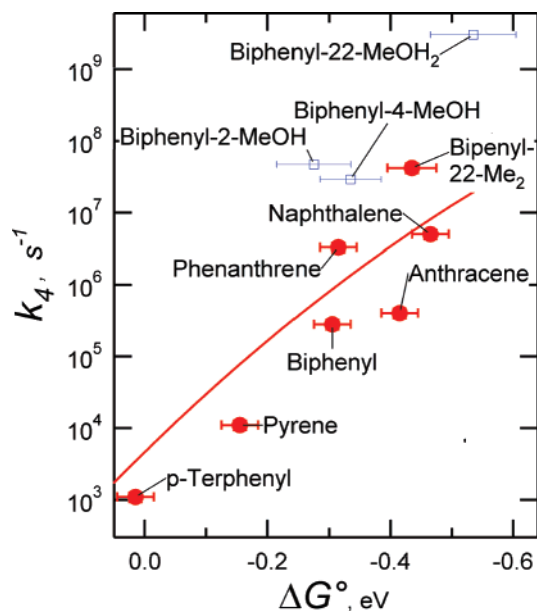

Figure 7. Free energy correlation for rate constants of Ar$^{\bullet-}$ protonation in ethanol (reaction 4). The values for $\Delta G°$ are calculated using eq 10 and data given in Table 2 with X taken as -0.28 eV. Still, the origin of the $\Delta G°$ axis remains uncertain and the actual values of $\Delta G°$ could be more negative. The line through the rate data is fit to the rate constants for compounds without MeOH substituents ($\bullet$) based on eqs 11−13 with $\nu = 3.6 \times 10^{10}$ s^{-1}, $\lambda = 1.41$ eV, and $T\Delta S° = -0.216$ eV. Faster rates for MeOH-substituted aryls ($\square$) may signal a change in mechanism (see the Discussion).

element, λ is a reorganization energy, and κ allows for nonadiabaticity. The activation free energy, $\Delta G^{\ddagger}$, enthalpy, and entropy are given by[28]

$$\Delta G^{\ddagger} = \frac{\lambda}{4}\left(1 + \frac{\Delta G°}{\lambda}\right)^2 \quad \text{and} \quad |\Delta G°| \leq \lambda \qquad (12)$$

$$\Delta H^{\ddagger} \cong \frac{\lambda}{4} + \frac{\Delta H°}{2}\left(1 + \frac{\Delta G°}{\lambda}\right) - \frac{(\Delta G°)^2}{4\lambda} \qquad (13)$$

$$\Delta S^{\ddagger} = \frac{\Delta S°}{2}\left(1 + \frac{\Delta G°}{\lambda}\right) \qquad (14)$$

We applied eqs 11−13 to the non-MeOH rate data in Figure 7

Protonation of Aryl Anions

J. Phys. Chem. B, Vol. 111, No. 24, 2007 **6901**

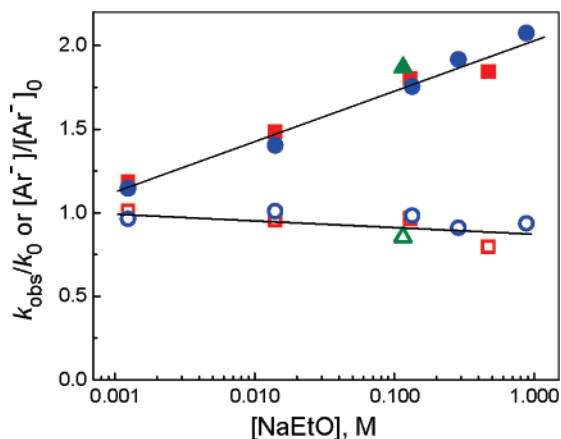**Figure 8.** Effect of NaEtO on the relative observed rate constant of $Ar^{\bullet-}$ decay via protonation (k_{obs}/k_0, open symbols) and on the dose-normalized relative concentration of produced $Ar^{\bullet-}$ ($[Ar^{\bullet-}]/[\,Ar^{-}]_0$, solid symbols). The subscript 0 marks the values measured in neat EtOH. *p*-Terphenyl, squares; pyrene, circles; biphenyl, triangles. The lines are given as visual aids only.

utilizing as parameters λ and the frequency factor, ν. To fit the experimental activation energies, we utilized in addition $T\Delta S°$ as a parameter, which defines $\Delta H°$. Global fitting to the data for non-MeOH aryls gave the results shown as a line in Figure 7 with $\nu = 3.6 \times 10^{10}$ s^{-1}, $\lambda = 1.41$ eV, and $T\Delta S° = -0.216$ eV. Inclusion of an adjustable offset in $\Delta G°$ produced a change of only 0.01 eV. A negative $T\Delta S°$ value is expected because it reflects the difference between the entropy for self-ionization of EtOH and the entropy for acid dissociation of $ArH^{\bullet}$ in EtOH. The $T\Delta S$ value for the former is -0.62 eV,[29] and although the entropy for the latter is not known, it should be much smaller due to a much more diffuse charge distribution on the highly delocalized MO in $Ar^{\bullet-}$ than on the localized MO in EtO^- with tight charge distribution; significantly more order is created by such a compression of charge in a polar solvent. Notably, the activation parameters for biphenyl (Table 4) are fairly reproduced by eqs 11, 13, and 14 and the fitted values for ν, λ, and $T\Delta S°$; the values log $A = 8.1$ and $E_a = 128$ meV are obtained.

The fitting procedure assumes that λ and $T\Delta S°$ are the same for all of the aryls, which is unlikely the case. Variations in λ and $\Delta S°$ will produce scatter. Much smoother free energy correlations were obtained when a series of acids were used to protonate a common aryl anion[4] or carbanion,[6] avoiding the larger changes in λ for various aryls. As has been explained by Eigen[30] and Marcus,[8] for the proton transfer reactions between O and C atoms, a carbon acid or base contributes the most to λ; the present work changes the carbon base, $Ar^{-\bullet}$. Another factor that could contribute to scatter is the variations in charge on the carbon atom being protonated; the negative charge will bring the EtOH proton closer.[31] Although MO coefficients vary by only ~25% among the aryl anions studied here, the rates may be extremely sensitive to proton transfer distance.

MeOH-Substituted Aryls. For comparable driving forces, anions of the MeOH-substituted biphenyls are protonated at rates one to two decades faster than those for unsubstituted aryls. Uncertainties in the free energy changes for these compounds are larger, as indicated in Figure 7. Not included in the uncertainties for the calculated driving forces are possible systematic errors in the computation of $ArH^{\bullet}$ dissociation, which is 0.1 eV smaller for all of the 2-substituted biphenyls (Table 2). If that 0.1 eV difference were absent, the scatter in Figure 7, especially for the MeOH-substituted biphenyls, would
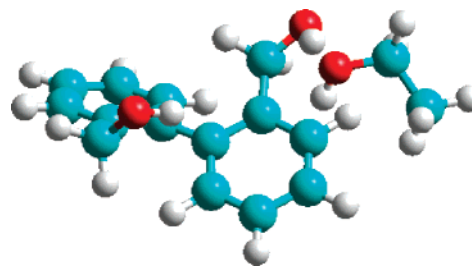
remain but would be reduced. While errors in the energetics might be larger than our estimates, such an explanation does not seem adequate, especially for the 3×10^9 s^{-1} rate seen in the anion of 2,2′-biphenyldimethanol. That rate is almost 100 times faster than the rate in 2,2′-dimethylbiphenyl, although there is no reason to expect large electronic differences in the π systems of these two molecules. The explanation that fast rates in these molecules are due to intramolecular proton transfer is difficult to reconcile with the small (or absent) rates of that process in THF (Table 3). Further, an exceptionally high rate is seen for 4-methanolbiphenyl in which intramolecular proton transfer does not seem possible.

For the MeOH-substituted biphenyls, an additional "solvent-assisted proton transfer" may also be available. The aryl MeOH groups in these molecules are expected to be stronger acids than the EtOH solvent on the basis of gas phase measurements.[32] If these MeOH groups participate in the hydrogen-bonded network that is typical of alcohols, it could donate a proton to a neighboring EtOH molecule, which could in turn donate a proton to the aryl ring. Free energy changes for this mechanism would be more negative than those in Table 2 and Figure 7. While we are not aware of measurements for the acidities of aryl MeOH groups in solution, deprotonation of benzyl alcohol is more favorable than that for EtOH by 0.3 eV in the gas phase.[32] A possible conformation in which this process might occur is shown in Figure 9.

In providing faster proton transfer, the solvent-assisted mechanism is likely to add some activation energy, which could explain the curious behavior of proton transfer in 2,2′-biphe-nyldimethanol. Despite its four decade larger rate compared to biphenyl, the activation energy is unexpectedly larger. The solvent-assisted mechanism is not established but is a conjecture which can accommodate the puzzling observations. If it is correct, then substantial departures of the MeOH-substituted biphenyls from the curve in Figure 7 could be due to this reaction channel, occurring in parallel with the same protonation by the solvent as with the other aryls (reaction 4).

Conclusions

Proton transfer rates from a single weak proton donor, ethanol, to a series of aromatic radical anions span a 6.5 decade range. The rate constants for molecules not having MeOH substituents correlate with free energy change in the conventional Marcus description of reorganization over the 0.5 eV range of $\Delta G°$. Variation of the aryls in the present study leads to scatter that may result from variations of reorganization energies and electron densities, but this variation is valuable in showing that two different contributions to the driving force, stability of the radical anions, as indicated by reduction potentials, and strengths of the $Ar-H$ bonds in the radicals, are both reflected in the rates. MeOH substituents, when present, somehow give sub-

stantially higher rates that may involve intramolecular proton transfer from the MeOH assisted by the hydrogen-bonded EtOH solvent molecules.

Supporting Information Available: Additional spectra of radical anions and ArH• radicals, computed dissociation energies for isomers of ArH• radicals, and detailed explanation of cycles used to compute energetics. This material is available free of charge via the Internet at http://pubs.acs.org.

References and Notes

(1) Arai, S.; Tremba, E. L.; Brandon, J. R.; Dorfman, L. M. *Can. J. Chem.* **1967**, *45*, 1119−1123.

(2) Dorfman, L. M. *Acc. Chem. Res.* **1970**, *3*, 224−230.

(3) Mazurkiewicz, K.; Haranczyk, M.; Gutowski, M.; Rak, J.; Radisic, D.; Eustis, S. N.; Wang, D.; Bowen, K. H. *J. Am. Chem. Soc.* **2007**, *129*, 1216−1224. Haranczyk, M.; Rak, J.; Gutowski, M.; Radisic, D.; Stokes, S. T.; Bowen, K. H. *J. Phys. Chem. B* **2005**, *109*, 13383−13391. Bachorz, R. A.; Haranczyk, M.; Dabkowska, I.; Rak, J.; Gutowski, M. *J. Chem. Phys.* **2005**, *122*. Bachorz, R. A.; Rak, J.; Gutowski, M. *Phys. Chem. Chem. Phys.* **2005**, *7*, 2116−2125. Dabkowska, I.; Rak, J.; Gutowski, M.; Nilles, J. M.; Stokes, S. T.; Radisic, D.; Bowen, K. H. *Phys. Chem. Chem. Phys.* **2004**, *6*, 4351−4357. Gutowski, M.; Dabkowska, I.; Rak, J.; Xu, S.; Nilles, J. M.; Radisic, D.; Bowen, K. H. *Eur. Phys. J. D* **2002**, *20*, 431−439.

(4) Jaworski, J. S. *J. Chem. Soc., Perkin Trans. 2* **1999**, 2755−2760. Jaworski, J. S.; Cembor, M. *Tetrahedron Lett.* **2000**, *41*, 7267−7270. Jaworski, J. S.; Cembor, M. *J. Phys. Org. Chem.* **2003**, *16*, 655−660.

(5) Peters, K. S.; Cashin, A.; Timbers, P. *J. Am. Chem. Soc.* **2000**, *122*, 107−113. Peters, K. S.; Kim, G. *J. Phys. Chem. A* **2001**, *105*, 4177−4181. Heeb, L. R.; Peters, K. S. *J. Phys. Chem. A* **2006**, *110*, 6408−6414.

(6) Andrieux, C. P.; Gamby, J.; Hapiot, P.; Saveant, J. M. *J. Am. Chem. Soc.* **2003**, *125*, 10119−10124.

(7) Marcus, R. A. *J. Phys. Chem.* **1968**, *72*, 891−899. Bell, R. P. *The Proton in Chemistry*; Chapman and Hall: London, 1973. Bell, R. P. *J. Chem. Soc., Faraday Trans. 2* **1976**, *72*, 2088−2094. Bell, R. P. *The Tunnel Effect in Chemistry*; Chapman and Hall: London, 1980. Mayer, J. M.; Hrovat, D. A.; Thomas, J. L.; Borden, W. T. *J. Am. Chem. Soc.* **2002**, *124*, 11142−11147. Anne, A.; Fraoua, S.; Grass, V.; Moiroux, J.; Saveant, J. M. *J. Am. Chem. Soc.* **1998**, *120*, 2951−2958.

(8) Marcus, R. A. *J. Phys. Chem.* **1969**, *91*, 7224−7225.

(9) Creutz, C.; Sutin, N. *J. Am. Chem. Soc.* **1988**, *110*, 2418−2427. Basilevsky, M. V.; Soudackov, A. V.; Vener, M. V. *Chem. Phys.* **1995**, *200*, 87−106. Basilevsky, M. V.; Vener, M. V.; Davidovich, G. V.; Soudackov, A. V. *Chem. Phys.* **1996**, *208*, 267−282. Lee, S.; Hynes, J. T. *J. Chim. Phys. Phys.-Chim. Biol.* **1996**, *93*, 1783−1807. Tran-Thi, T. H.; Gustavsson, T.; Prayer, C.; Pommeret, S.; Hynes, J. T. *Chem. Phys. Lett.* **2000**, *329*, 421−430. Kiefer, P. M.; Hynes, J. T. *Solid State Ionics* **2004**, *168*, 219−224. Kiefer, P. M.; Hynes, J. T. *Isr. J. Chem.* **2004**, *44*, 171−184. Kiefer, P. M.; Hynes, J. T. *J. Phys. Chem. A* **2004**, *108*, 11809−11818. Kiefer, P. M.; Hynes, J. T. *J. Phys. Chem. A* **2004**, *108*, 11793−11808. Kiefer, P. M.; Hynes, J. T. *J. Phys. Chem. A* **2003**, *107*, 9022−9039. Kiefer, P. M.; Hynes, J. T. *J. Phys. Chem. A* **2002**, *106*, 1850−1861. Kiefer, P. M.; Hynes, J. T. *J. Phys. Chem. A* **2002**, *106*, 1834−1849.

(10) Olmstead, W. N.; Margolin, Z.; Bordwell, F. G. *J. Org. Chem.* **1980**, *45*, 3295−3299. Bordwell, F. G.; Liu, W. Z. *J. Am. Chem. Soc.* **1996**, *118*, 10819−10823.

(11) Parker, V. D.; Tilset, M.; Hammerich, O. *J. Am. Chem. Soc.* **1987**, *109*, 7905−7906.

(12) Freeman, G. R. *Radiation Chemistry of Ethanol: A Review of Data on Yields, Reaction Rate Parameters, and Spectral Properties of Transients*; U.S. Department of Commerce: Washington, DC, 1974.

(13) Caldin, E. F.; Long, G. *J. Chem. Soc.* **1954**, 3737−3742.

(14) Wishart, J. F.; Cook, A. R.; Miller, J. R. *Rev. Sci. Instrum.* **2004**, *75*, 4359−4366. Wishart, J. F. In *Radiation Chemistry: Present Status and Future Trends*; Jonah, C. D., Rao, B. S. M., Eds.; Elsevier Science: Amsterdam, The Netherlands, 2001; Vol. 87, pp 21−35.

(15) Miller, J. R.; Penfield, K.; Johnson, M.; Closs, G.; Green, N. In *Photochemistry and Radiation Chemistry. Complementary Methods for the Study of Electron Transfer*; Wishart, J. F., Nocera, D. G., Eds.; American Chemical Scoiety: Washington, DC, 1998; Vol. 254, pp 161−176.

(16) Akhtar, S. M. S.; Freeman, G. R. *J. Phys. Chem.* **1971**, *75*, 2756−2762. Jha, K. N.; Freeman, G. R. *J. Chem. Phys.* **1972**, *57*, 1408−1414. Rabani, J.; Gratzel, M.; Chaudhri, S. A. *J. Phys. Chem.* **1971**, *75*, 3894−3894.

(17) Allen, A. O. *Yields of Free Ions Formed in Liquids by Radiation*; U. S. Government Printing Office: Washington, DC, 1976.

(18) Computations performed with Gaussian 98 (revision A.7): Frisch, M. J.; Trucks, G. W.; Schlegel, H. B.; Scuseria, G. E.; Robb, M. A.; Cheeseman, J. R.; Zakrzewski, V. G.; Montgomery, J. A., Jr.; Stratmann, R. E.; Burant, J. C.; Dapprich, S.; Millam, J. M.; Daniels, A. D.; Kudin, K. N.; Strain, M. C.; Farkas, O.; Tomasi, J.; Barone, V.; Cossi, M.; Cammi, R.; Mennucci, B.; Pomelli, C.; Adamo, C.; Clifford, S.; Ochterski, J.; Petersson, G. A.; Ayala, P. Y.; Cui, Q.; Morokuma, K.; Malick, D. K.; Rabuck, A. D.; Raghavachari, K.; Foresman, J. B.; Cioslowski, J.; Ortiz, J. V.; Stefanov, B. B.; Liu, G.; Liashenko, A.; Piskorz, P.; Komaromi, I.; Gomperts, R.; Martin, R. L.; Fox, D. J.; Keith, T.; Al-Laham, M. A.; Peng, C. Y.; Nanayakkara, A.; Gonzalez, C.; Challacombe, M.; Gill, P. M. W.; Johnson, B. G.; Chen, W.; Wong, M. W.; Andres, J. L.; Head-Gordon, M.; Replogle, E. S.; Pople, J. A. *Gaussian 98*, revision A.7; Gaussian, Inc.: Pittsburgh, PA, 1998.

(19) Lee, C.; Yang, W.; Parr, R. G. *Phys. Rev. B* **1988**, *37*, 785−789. Becke, A. D. *J. Chem. Phys.* **1993**, *98*, 5648−5652. Johnson, B. G.; Gill, P. M. W.; Pople, J. A. *J. Chem. Phys.* **1993**, *98*, 5612−5626.

(20) Shida, T. *Electronic Absorption Spectra of Radical Ions*; Elsevier Science Publishers B.V.: Amsterdam, The Netherlands, 1988.

(21) Arai, S.; Dorfman, L. M. *J. Chem. Phys.* **1964**, *41*, 2190−2194. Watson, E.; Roy, S. *Selected Specific Rates of Reactions of the Solvated Electron in Alcohols*; U.S. Department of Commerce: Washington, DC, 1974.

(22) Fendler, J. H.; Gillis, H. A.; Klassen, N. V. *J. Chem. Soc., Faraday Trans. 1* **1974**, *70*, 145−153.

(23) Streitwieser, A.; Schwager, I. *J. Am. Chem. Soc.* **1962**, *66*, 2316−2320. Zachariasse, K. A. Chemiluminescence from Radical Ion Recombination. Ph.D. Thesis, 1972.

(24) Meerholz, K.; Heinze, J. *J. Am. Chem. Soc.* **1989**, *111*, 2325−2326.

(25) Berho, F.; Rayez, M.-T.; Lesclaux, R. *J. Phys. Chem. A* **1999**, *103*, 5501−5509.

(26) Fletcher, J. W.; Richards, P. J.; Seddon, W. A. *Can. J. Chem.* **1970**, *48*, 1645−1650.

(27) Peon, J.; Polshakov, D.; Kohler, B. *J. Am. Chem. Soc.* **2002**, *124*, 6428−6438.

(28) Marcus, R. A.; Sutin, N. *Biochim. Biophys. Acta* **1985**, *811*, 265−322.

(29) Jolly, W. L. *J. Am. Chem. Soc.* **1952**, *74*, 6199−6201.

(30) Eigen, M. In *Nobel Symposium No. 5; Fast Reactions and Primary Processes in Chemical Kinetics*; Claesson, S., Ed.; Interscience: New York, 1967; pp 245−253.

(31) Sutin, N. Personal communication.

(32) Bartmess, J. E.; Scott, J. A.; McIver, R. T. *J. Am. Chem. Soc.* **1979**, *101*, 6046−6056.